Delta-Sigma Oversampled Ultrasound Beamformer with Dynamic Delays

Steven R. Freeman, *Member, IEEE*, Marshall K. Quick, Marc A. Morin, *Member, IEEE*, R. Carver Anderson, Charles S. Desilets, *Member, IEEE*, Thomas E. Linnenbrink, *Member, IEEE*, and Matthew O'Donnell, *Fellow, IEEE*

***Abstract*—The principles of oversampling are exploited in a simple beamforming architecture using a single bit delta-sigma ($\Delta\Sigma$) analog to digital converter (A/D) on every channel. The high sampling rate required for the single bit A/D provides adequate delay accuracy for high quality beamforming using elementary sample manipulations. Images produced with this beamformer exhibit significant artifacts directly related to dynamic focusing. However, a simple digital recoding technique following delays permits dynamically focused beamforming without degrading image quality. The simplicity of this beamformer compared to conventional methods may facilitate very large channel count or low power beamformers suitable for 1.5-D arrays or portable scanners.**

I. Introduction

Ultrasound imaging changes with the state-of-the-art in electronics [1]. In the 1970s, B-scans were generated using mechanical scanning of a single element transducer [2]. A clinically useful image was generated by varying the intensity of an appropriately scanned CRT beam; more sophisticated systems interpolated the CRT image. Later, Doppler processing was added by stopping the motion of the imaging transducer so a single line could be interrogated repeatedly. Analog processing techniques were used for envelope detection, Doppler estimation, and display control because digital techniques were still too slow and expensive. Due to the fixed transmit and receive focus of these systems, image quality was marginal.

By the 1980s, phased array systems were made possible by advances in analog delay lines and the reduced size of analog processing elements. Some systems were limited to fixed-focus receive operations because the noise introduced by changing delay line taps adversely affected image quality. Others synthesized several focal zones using expensive, finely tapped delay lines that injected little noise when switched [3]. In 1979 Maslak [4], then at Hewlett Packard, patented a method for dynamic delays without changing delay taps. By heterodyning the RF signal from each channel to an intermediate frequency, a phase manipulating circuit could perform fine delay changes, and a coarse delay line held a large constant delay. In this way, the imaging system created multiple receive foci without expensive ultra-low noise delay lines.

In the late 1980s, advances in analog-to-digital conversion led many manufacturers to perform more beamformer processing digitally. Dynamic delay changes were implemented by one of three techniques. The first required an analog or digital modulation of the RF signal to an intermediate frequency or baseband [5], [6]. If the modulation was analog, a slower (cheaper) A/D could be used due to the reduced carrier frequency. If the A/D could support sampling rates four times the carrier, appropriate decimation of the digital samples yielded the in-phase (I) and quadrature (Q) components of a baseband signal. In either case, dynamic delays could be implemented digitally using phase rotation circuitry, and digital FIFOs could produce large fixed delays. This technique closely approximates the system proposed by Maslak [4], except that the rotation and delays were implemented digitally with 8-12 bit precision.

The second dynamic digital delay technique used an interpolation filter to effectively up-sample the incoming digital sample stream to acquire the appropriate finely delayed samples [7], [8]. Different filters were required for each intersample delay. The third technique involved nonuniform sampling of the RF signal on each channel according to the desired delay [9], [10]. All three approaches are used in state of the art machines. Due to the high precision and low noise of these beamformers, images of superior quality are possible. In addition, many advanced functions can be added to the imager using digital signal processing hardware to generate high quality spectral Doppler, color flow, and power Doppler measurements, or to perform phase aberration correction.

Although digital beamforming is well established, its complexity makes large channel count machines difficult to design. Most state-of-the-art imaging systems have 128 to 256 channel beamformers that produce exquisite 2-D images of a single tissue plane. For volumetric scans (3-D) or spatial compounding, the imaging plane must be steered using a 1.5-D or 2-D transducer array [11]–[13].

Manuscript received January 26, 1998; accepted September 22, 1998. This work was supported in part by DARPA Contract No. N00014-96-C-0191 and also by Department of the Army Contract No. DAMD17-96-C-6037.

S. R. Freeman and M. O'Donnell are with the Electrical Engineering and Computer Science and Biomedical Engineering Departments, University of Michigan, Ann Arbor, MI 48109-2125 (e-mail: odonnel@eecs.umich.edu).

M. K. Quick, M. A. Morin, and T. E. Linnenbrink are with Q-DOT Incorporated, Colorado Springs, CO 80907-3579.

R. C. Anderson and C. S. Desilets are with Ultrex Corporation, Edmonds, WA 98020.

0885–3010/99$10.00 © 1999 IEEE

Luxottica et al. v. Solos
IPR2026-00412
Petitioners' Ex. 1019

These arrays require anywhere from 512 to 16,384 parallel processing channels. Sparse array geometries are being investigated widely to reduce this channel count [14], [15]; however, image quality usually suffers as a result of these subsampling techniques. Simplifying the beamforming hardware, therefore, is the most feasible method to develop economical 3-D scanners with large channel count beamformers. This paper describes a significant departure from traditional methods with the potential to dramatically reduce the size, complexity, and power consumption of the digital beamformer.

Oversampling A/Ds have become increasingly popular in digital processing applications because of their relative simplicity and ease of integration into other processing elements [16], [17]. Reduced feature size and increased density in state-of-the-art CMOS fabrication facilities have yielded microprocessors capable of 300 MHz operation. Oversampling A/Ds at such high frequencies could easily eliminate the complicated digital delay issues discussed here. This led us to investigate a delta-sigma modulator-based technique that can dramatically reduce the size, and ultimately the cost, of ultrasound digital beamformers and facilitate 3-D ultrasound imaging.

A dynamic receive beamformer developed by General Electric and patented in 1993 [18] used a delta-sigma oversampling A/D with simple digital processing schemes for the delay and coherent summation of the digitized ultrasound RF signal. A beamformer using oversampling A/Ds was patented later for radar applications [19]. In this paper we present the beamforming technique developed by General Electric and describe how it will reduce the power consumption and size of receive beamforming circuitry. Unfortunately, the beamformer as proposed suffers from a major flaw that significantly reduces image quality. We will present a method that completely corrects this flaw so that images of superior quality may be obtained. Ultrasound scans also will be presented that compare the image quality of the proposed system with that of traditional multi-bit digital beamforming techniques. A future paper will present a technique that further improves this system's sensitivity for narrowband applications (e.g., spectral Doppler measurements).

II. Delta-Sigma Modulation

Oversampling analog to digital converters (ADCs or A/Ds) are an efficient means of transforming an analog voltage into a digital representation because of their relative simplicity and ease of integration into other digital processing circuits [17]. Conventional, multi-bit A/Ds require analog filters and high-precision analog circuits susceptible to noise and process variations. Oversampling A/Ds, however, use simple, imprecise analog circuits operating at very high speeds to achieve sufficient signal-to-quantization noise ratios (SQNR). These A/Ds also can be implemented with standard VLSI (CMOS or BiCMOS) circuits easily incorporated onto the same chip as a microcontroller or digital signal processor, thereby eliminating the need for expensive interconnect and packaging. Because high sampling rates are needed, oversampling A/Ds primarily have been used in low frequency applications such as audio and instrumentation processing. As VLSI circuits become faster (e.g., the 500 MHz DEC Alpha microprocessor [20]), oversampling converters can be used in higher frequency systems such as communications, radar, video, and ultrasound. Here we explore these simple and fast single bit A/Ds to digitize incoming ultrasound RF signals, and later process their single-bit digital outputs to perform dynamic receive beamforming. This section introduces delta-sigma oversampling methods and discusses their use in a proposed beamforming architecture.

The quantization noise power of a traditional multi-bit A/D is approximately:

$$n_o^2 = \frac{e_{\text{rms}}^2}{\text{OSR}}, \tag{1}$$

where e_{rms}^2 is the mean squared value of the quantization error and OSR is the oversampling ratio, defined as the ratio of the sampling frequency to the Nyquist rate of the input signal [17]. The value of e_{rms}^2 is $\Delta^2/12$ assuming the error can be represented as uniformly distributed white noise, where Δ is the quantization interval. These well-known relations show that in-band noise can be decreased by 3 dB for each doubling of the sampling rate. A 1/2 bit resolution change on a multi-bit A/D also represents a 3 dB change in the quantization noise. A constant SQNR is possible, therefore, by doubling the sampling rate and reducing the bit length of the quantizer by 1/2 bit. An extension of this would be to increase the sampling rate sufficiently that a single-bit quantizer could maintain an adequate signal-to-quantization noise ratio. Such a quantizer could be implemented as a simple comparator, and downstream processing elements could operate on the single-bit output. The problem is that a significant increase in sampling rate is necessary ($2^{16} = 65{,}536$ times for an 8-bit quantizer), thus precluding the use of traditional (simple) circuitry, except for very low frequency signals. Other methods must be used so that a realistic sampling rate increase can generate a useful single-bit output.

A delta-sigma (also called a sigma-delta) modulator is an efficient oversampling A/D converter [17]. It uses one or more integration stages within a feedback path, as shown in Fig. 1(A), such that a two-level quantizer output tracks the average input. The difference between quantizer output and modulator input accumulates in the integrator and ultimately corrects itself so that the averages are equivalent. Assuming again that the quantizer introduces white noise, an equivalent linearized discrete-time model can be drawn for a first order delta-sigma modulator, as shown in Fig. 1(B). Using this model, the discrete-time system equation is:

$$D_q(z) = z^{-1}X(z) + [1 - z^{-1}]E(z). \tag{2}$$

Therefore, the output $D_q(z)$ is a summation of a delayed input $X(z)$ and high-pass filtered quantization noise, $E(z)$.

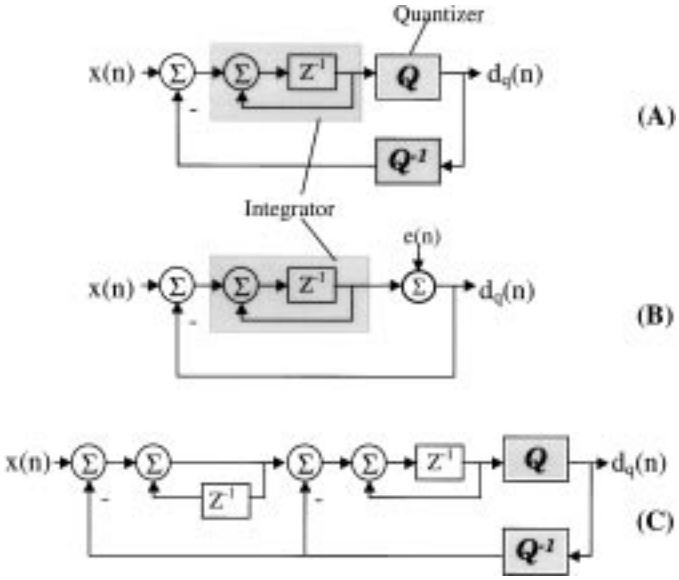

Fig. 1. (A) Block diagram of a first order delta-sigma modulator. (B) Equivalent discrete-time circuit diagram with white noise source, $e(n)$, replacing quantizer (Q) and DAC (Q^{-1}). (C) Block diagram of a second order delta-sigma modulator.

This noise shaping within the delta-sigma modulator is key to its success. By increasing the sampling rate, the band-edge of the input signal approaches the discrete-time zero frequency (DC), where the noise filter has its null. Therefore, large oversampling rates provide significant quantization noise reduction within the band of the input signal because so much of that noise is shifted to higher frequencies. The quantization noise power of this low-pass modulator is approximately [17]:

$$n_0^2 = e_{\mathrm{rms}}^2 \frac{\pi^2}{3} \left(\frac{1}{\mathrm{OSR}}\right)^3. \tag{3}$$

A doubling of the oversampling ratio (OSR) reduces the noise power by 9 dB, or 1.5 equivalent bits.

Higher order delta-sigma converters provide even better noise shaping abilities by inserting additional integrators into the feed-forward path. A second order modulator, shown in Fig. 1(C), improves SQNR by 15 dB for every doubling of the sampling rate. Similarly, a third order improves it by 21 dB. Although the circuit complexity increases slightly, they can still be implemented in relatively imprecise CMOS or BiCMOS technology. Third order and higher $\Delta\Sigma$ converters are not inherently stable. Modified structures, however, such as 2-1 cascades, provide stable third order performance with elevated circuit complexity [17], [21]. Signal conditioning within the converter also can reduce the likelihood that a traditional third order converter will enter an unstable state. Multi-level quantizers (rather than bi-level or single bit quantizers) also provide enhanced stability and improved performance.

Earlier, we assumed for simplicity that the quantization noise was white and uncorrelated with the input signal. This is not the case, however, and much literature has been generated attempting to characterize the noise of delta-sigma modulators [17], [22]. Tonal components in the frequency spectrum are pronounced and can change the SQNR of the system within the band of the signal. Fig. 2(A) shows a 3.5 MHz, 30% bandwidth ultrasound pulse reflected from several wires in a water tank. Fig. 2(B) shows the frequency spectrum for this signal sampled with a bi-level, second order delta-sigma A/D operating at 111 MHz. The quantization noise peaks at $\pi/2$ and $-\pi/2$ represent significant tonal components arising from low intensity signals between the wires.

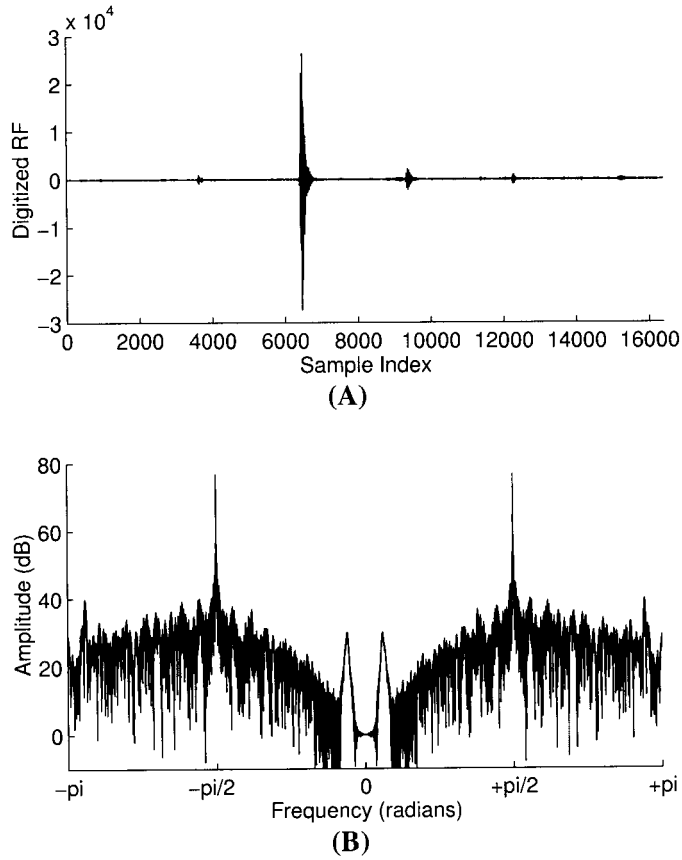

Fig. 2. (A) RF signal from 3.5 MHz, 30% bandwidth transducer insonifying wire target phantom. (B) Frequency spectrum of the signal in (A) after digitization by a 111 MHz second order $\Delta\Sigma$ modulator.

Reconstruction of the delta-sigma modulated signal requires a low-pass filter that cuts off quantization noise above the input signal band [17]. This filter usually is implemented digitally and yields multi-bit outputs. Decimation of the filtered signal then yields a low rate digital output comparable to multi- bit A/D outputs.

III. Receive Beamforming

A. Traditional Method

Considerable processing is required within an ultrasound machine to generate clinically useful images. High-end ultrasound scanners today generally use 128 processing channels connected to a transducer array to transmit high frequency sound pulses into the body and sense re-

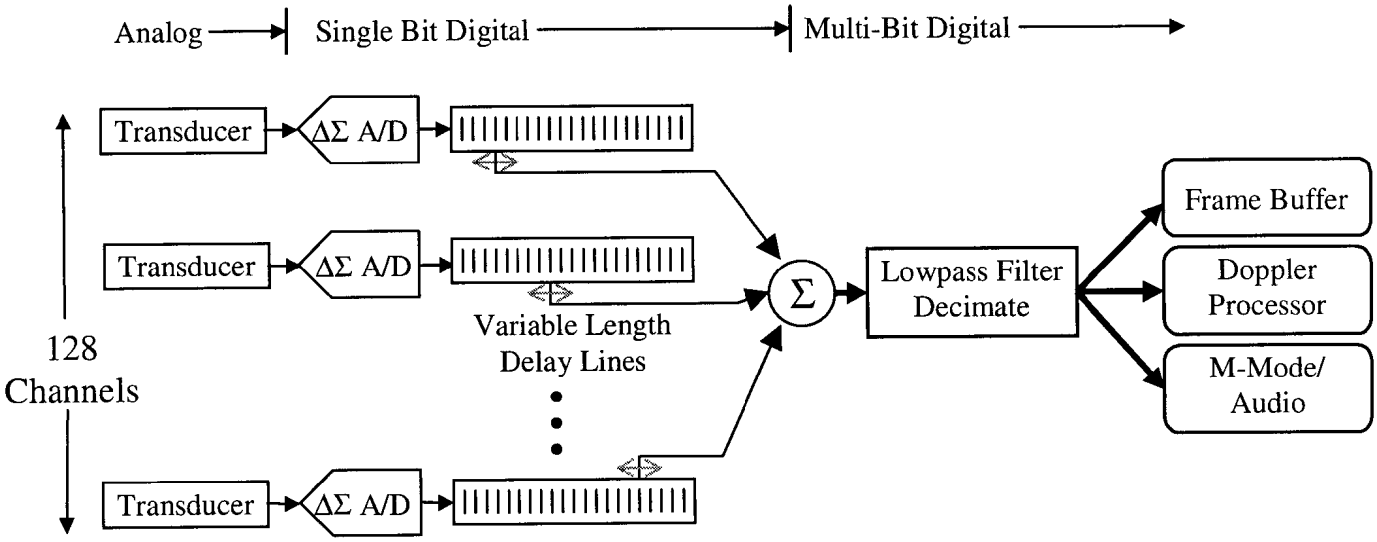

Fig. 3. Block diagram of a $\Delta\Sigma$ based receive beamformer.

flections returning from the tissue under observation [23]. More specifically, during transmission drive circuitry appropriately delays pulse excitation of each element in the array so that coherent interference occurs at a fixed distance from the transducer. On receive, digital delay and processing circuitry applies changing (dynamic) delays to each channel so that a coherent summation of the received signals generates a focus at many points along a particular direction of interest (i.e., a beam). Changing the delays on transmit and receive allows the system to change the direction of a particular beam so that many angles are interrogated within a plane coincident with the array. Once a sufficient number of beams has been acquired along different "looklines" in a frame, a reconstructed image is displayed to the user. Receive beamforming, though conceptually simple, requires considerable signal-processing capacity made available through many high speed application-specific integrated circuits (ASICs). In the following section, we discuss the processing and hardware requirements for dynamic receive beamforming, and later propose an alternative method significantly simplifying these processing elements by reducing their bit width.

Typical ultrasound scanners use a separate high speed (flash) 8–10 bit A/D at every channel on receive to digitize the incoming RF signal. (Analog amplification and time-gain compensation, TGC, is usually applied prior to digitization.) The A/Ds run at about 40 MHz and each consumes from 30 to several hundred milliwatts of power (e.g., Philips' TDA8790[1] or Analog Devices' AD9048 or AD9040[2]). A 10-bit flash A/D, for instance, has 1,024 comparators connected to a biasing network to encode the input voltage. The overall precision of the A/D is set by the precision of the comparators and biasing, which is also related to the power consumption of these circuits. Their size and integration with downstream processing is also a significant problem. The A/Ds usually are packaged individually in multichip modules, so integrating them with other circuitry requires space-consuming interconnect on printed circuit boards. Monolithically integrating the A/D and digital delay processing circuitry for many channels on the same chip is a significant challenge.

Following digitization, delays (τ_n) are applied to generate a dynamic receive focus. For a conventional sector scan, where the beam always intersects the array at its center, the delay as a function of range (in the limit that the f/number of the aperture is approximately 2 or greater) is:

$$\tau_n \cong -\frac{x_n^2 \cos^2 \Theta}{2Rc} + \frac{x_n \sin \Theta}{c} + \text{constant}, \tag{4}$$

where x_n is the distance from each element to the center of the array, Θ is the steering angle, c is the sound speed in the medium, and the range R is the range from the array center. The constant in (4) is applied to obtain only positive delays across the array. Because range is simply related to elapsed propagation time, t, from transmit as $2R = ct$ in pulse-echo imaging, the dynamic delay equation can be expressed as an explicit function of time:

$$\tau_n \cong -\frac{x_n^2 \cos^2 \Theta}{c^2 t} + \frac{x_n \sin \Theta}{c} + \text{constant}. \tag{5}$$

The first (quadratic) term focuses the beam to a particular range, whereas the second (linear) term steers the beam off axis. These delays have a 1/range ($1/t$) dependence and should be accurate to about 1/32 of a wavelength ($\lambda/32$) to maintain an accurate focus [19], [24], [25]. Because the sampling rate of the A/D is usually about four to eight times the ultrasound carrier frequency, this accuracy cannot be met simply by repeating or dropping digitized samples. As a result, two methods are commonly used to accurately delay digitized signals.

The first uses basebanding and phase rotations to achieve inter-sample delay accuracy [6]. Here the RF sig-

[1] Philips Semiconductor Product Specification, Integrated Circuits, February 21, 1996.

[2] Analog Devices Design-In Reference Manual, 1994.

nal is simultaneously modulated with cosine and sine functions to produce a complex baseband signal, containing in-phase (I) and quadrature-phase (Q) components. A common trick is to choose the sampling rate as exactly four times the carrier frequency so that cosine and sine modulation can be implemented as a simple zero and signed unity multiplier. Appropriate filtering and decimation yields the I and Q components. Once the complex baseband signal has been created, each sample is then rotated through an arbitrary angle for precise delays. This rotation can be performed by a multi-stage pipelined CORDIC processor [6], [26]. Coarse delays are achieved by simple digital delays (e.g., FIFOs) operating at the decimated sampling rate on these phase adjusted complex signals.

The second method applies a sinc interpolation filter and decimation of the interpolated sample sequence to finely adjust digital delays [7], [8]. Each of the possible inter-sample delays requires a different FIR filter operating on many incoming data samples. Massively parallel processing is required to multiply the appropriate samples with filter weights and perform the summation for each output sample.

Both methods can achieve highly accurate delays using rather coarse sampling intervals, but they require substantial processing. Also, remember that each channel must have its own individual delay circuitry, so as channel count increases the complexity and size of the circuit increases accordingly. Power consumption and size of the receive beamforming circuitry are largely the result of these fine delay processing elements. Simplification of the delay operation will considerably reduce the power consumption and size of the beamformer (see Section III,B).

The final stage in the receive beamforming process sums the delayed samples across the array. Each sample, having been appropriately delayed, enters a pipelined adder that spans the width of the array and generates a "beam sum". These adders are usually at least 16 bits in width and operate at the sample rate of the A/Ds (or at the slower baseband decimated rate). In the case of baseband signals, the summation is actually a complex number addition yielding complex outputs, whereas the interpolate/decimate method yields real integer outputs. Summer outputs are stored in a memory buffer and later scan converted for display to the user, or are manipulated in co-processing elements such as Doppler processors.

B. Delta-Sigma Modulator Method

Multi-bit digital beamforming techniques produce high quality ultrasound images. Similar image quality can be obtained using oversampling techniques, but with dramatic reduction in complexity and size. A delta-sigma based dynamic receive beamformer, for instance, yields two important benefits over traditional multi-bit methods. First, the A/D itself is more easily integrated onto the same chip as the processing circuitry creating the beam. Thus, interconnect, size, and power consumption are reduced. Second, accurate delays can be achieved simply by manipulating individual samples at the high sampling rate. The complicated basebanding or interpolate/decimate circuits may be replaced by a variable length shift register determining the delay of the signal prior to summation. The sum across the array also can be replaced by a series of full adders running at high speed. The block diagram of a delta-sigma based receive beamformer, as first proposed in [18], is shown in Fig. 3.

Due to the large dynamic range necessary for ultrasound applications, the $\Delta\Sigma$ A/D must be a second or third order modulator to maintain adequate signal-to-noise ratio. A fourth order band-pass delta-sigma modulator has even been proposed in [27] for ultrasound imaging. A sampling rate of 32 times the carrier or higher is chosen to provide both high signal-to-noise ratio and adequate delay accuracy. The quantizer at the output of the modulator is usually a two-level quantizer because of its simplicity. Adding more levels to the quantizer improves the SQNR of the system but considerably complicates the analog feedback circuitry. Cascaded forms of high order $\Delta\Sigma$ A/Ds use multiple two-level quantizers and digital filtering to generate a multi-level digital output without the need for complicated multi-level quantizers [17]. Such cascaded $\Delta\Sigma$ A/Ds complicate downstream processing, however, due to the increased output bit width.

The digital output of the modulator enters a variable length digital delay line, or shift register, that applies dynamic delays to the signal. This shift register must operate at the sampling frequency and contain several hundred stages to accommodate the net dynamic delay change over the period of every beam. The actual length of the delay line depends on many factors, including sampling rate, array geometry, steering angle, maximum imaging depth, and carrier frequency. The size and power consumption of this delay line is very similar to those in traditional beamformers because the sample rate is about eight times faster (320 vs. 40 MHz) but the bit width is at least eight times smaller (1 bit vs. 8-10 bit). When the length of the delay line changes to produce a new focal zone, samples must be repeated, inserted, or dropped at the input, output, or even in the middle of the shift register. The control circuitry on every channel in this $\Delta\Sigma$ beamformer is roughly equivalent to that in conventional systems.

Delayed samples are then summed, digitally, across the array to form a beam. This summation must occur at the sampling rate of the A/Ds, and requires a pipelined set of digital adders across the array. Once the beam sum has been generated, a steep-rolloff (high-order) low-pass filter is applied to the beamformed samples to cut off $\Delta\Sigma$ quantization noise. Because only one such filter is required per beam sum, it can be very long and complicated and consume a fair amount of power. Decimation of the filtered sample stream lowers the sampling rate considerably, thereby allowing traditional downstream processing elements to be used. Envelope detection, scan conversion, Doppler processing, and display can all be accomplished by traditional methods.

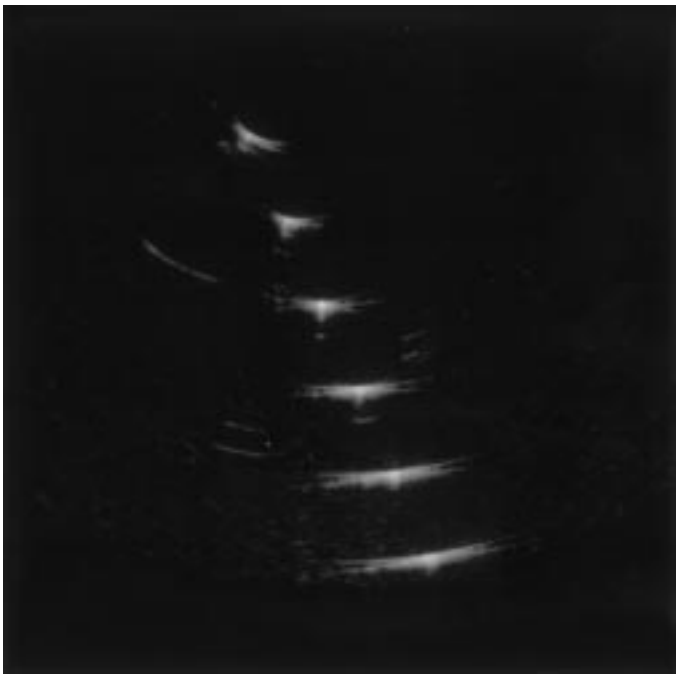

Fig. 4. Ten-bit A/D-delay-sum beamformer with dynamic focusing. Target: wire phantom.

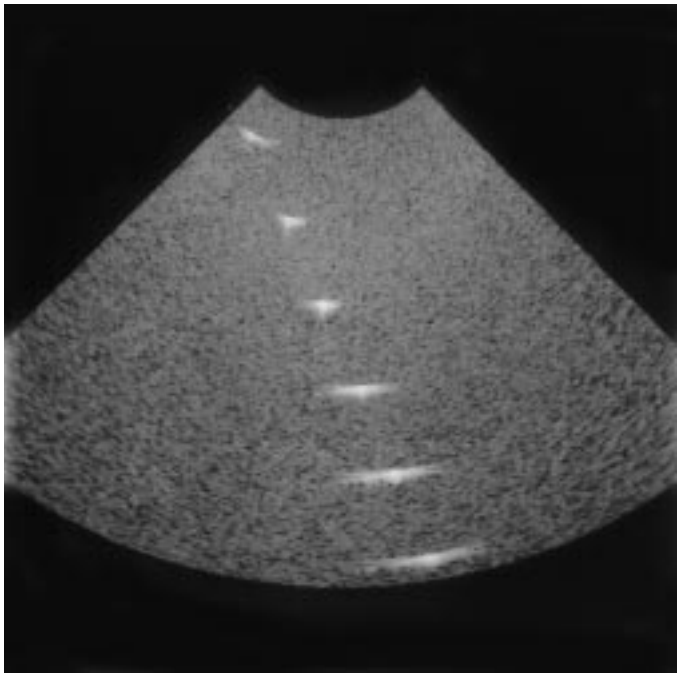

Fig. 5. Uncompensated $\Delta\Sigma$-delay-sum beamformer with dynamic focusing. Target: wire phantom.

IV. The Problem

The $\Delta\Sigma$-based beamformer presented here was emulated in software using real ultrasound data collected in our laboratory (available over the World Wide Web at http://bul.eecs.umich.edu). The emulations showed that this dynamically focused beamformer produced images of surprisingly poor quality compared to conventional multibit beamforming methods. Fig. 4 shows a 3.5 MHz, 90 degree sector image of six wires in a water tank using a 10-bit A/D per channel conventional beamformer. The depth of this 70 dB dynamic range image is 160 mm. Comparing this to Fig. 5, generated by the $\Delta\Sigma$-based beamformer, the noise floor was considerably higher than expected (by almost 20 dB). Further investigation revealed that the dynamic delay changes were directly responsible for the noise increase. When the $\Delta\Sigma$-based beamformer imposed a fixed focus on transmit and receive (i.e., no delay changes) it produced images comparable to conventionally beamformed images in the same operating mode; see Figs. 6 and 7 displayed over the same 70 dB dynamic range. This apparent flaw in the $\Delta\Sigma$ beamformer has been corrected so that images of superior quality result. Here we discuss the nature of the flaw as well as its compensation. Later, ultrasound images will be shown that illustrate the effectiveness of correctly changing the delays or compensating the modulator.

The $\Delta\Sigma$ A/D and low-pass reconstruction filter shown in Fig. 3 constitute a modulator-demodulator pair. Linear time-invariant systems or operations can be inserted between the modulator and demodulator without degrading effects. The summation across the array is an example of this, where the modulated signal is summed and

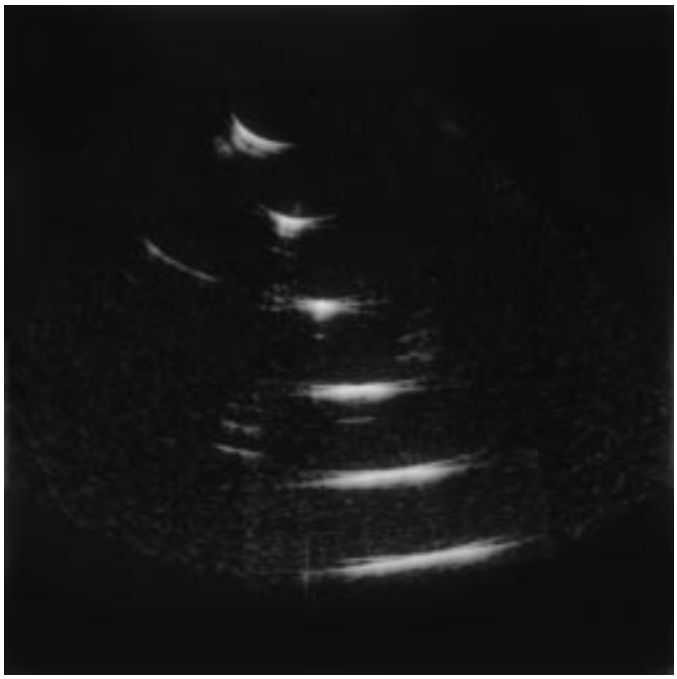

Fig. 6. Ten-bit A/D beamformer with fixed focus at 60 mm. Target: wire phantom.

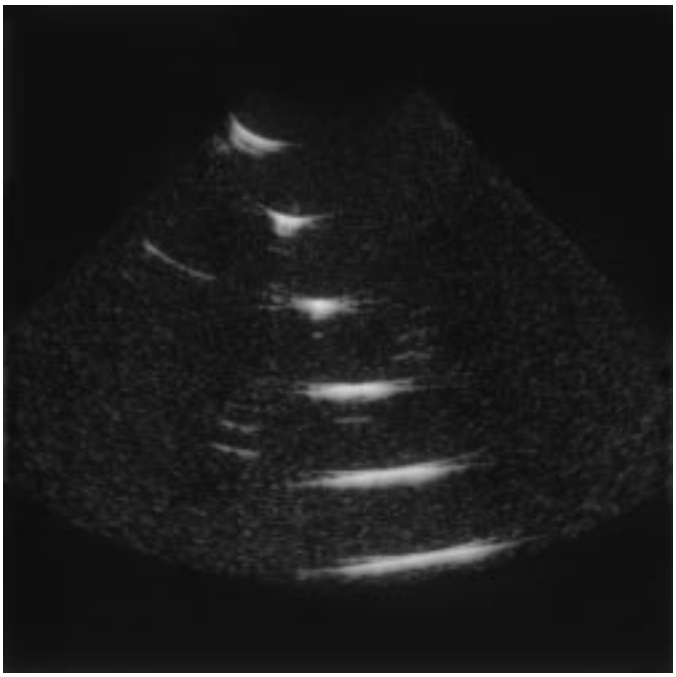

Fig. 7. Uncompensated ΔΣ-delay-sum beamformer with fixed focus at 60 mm (3rd wire from top). Target: wire phantom.

later reconstructed (filtered). The time-variant operation of repeating (or deleting) samples in the delay line, however, disrupts synchronization between modulator and demodulator. Under normal operation, running differences in the modulator are canceled within the demodulator filter, thus producing a faithful representation of the input signal. The demodulator filter interprets an extra sample (or withdrawn sample) as an extra difference from the modulator which did not actually exist. The filter thus injects (or passes) extra energy into the output signal not present in the input.

V. The Solution

There are three ways of stretching the sample stream in the delay structure (i.e., increasing the delay): repeating a sample, inserting an effective zero sample, or splitting it into two equal parts. The previous section has described the undesirable consequences of repeating a sample. One simple solution is to force the modulator to take the repeated (or dropped) sample into account in its operation, and, therefore, in the modulation of the ensuing sample stream. To do this, a multiplexer is inserted into the feedback loop choosing between a zero, normal, or scaled-by-two magnitude. Samples later repeated in the delay structure must have a feedback magnitude of two because each sample is encountered twice at the demodulator. Those samples dropped within the delay structure need to have a feedback magnitude of zero because they will never be seen by the demodulator. Finally, normal, nonrepeated samples must have unity feedback. This type of modulator, which includes the feedback multiplexer as shown in Fig. 8(A),

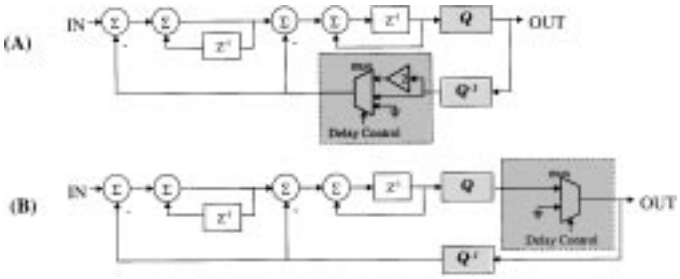

Fig. 8. (A) Block diagram of compensated second order ΔΣ analog to digital converter when delay change requires repetition (for extension) or skipping (for compression) of the output sample. (B) Block diagram of a compensated ΔΣ A/D when delay change requires skipping or summing (for compression) of the output sample.

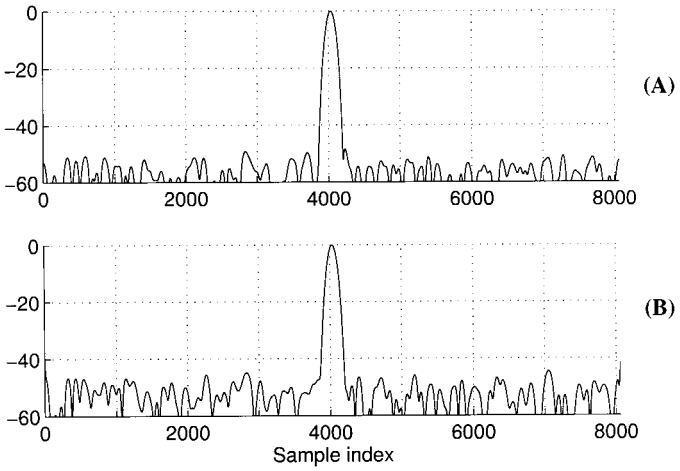

Fig. 9. (A) A 3.35 MHz detected baseband pulse with −50 dB added noise. (B) Reconstructed and detected signal after digitization by a 2nd order ΔΣ modulator running at 214 MHz.

will be referred to as a compensated delta-sigma modulator.

The other two methods of dynamically changing focusing delays are easier to implement. In these cases where the sample is split into two equal parts or a zero is inserted, nothing is done within the modulator to compensate the sample series. These methods do not affect the average signal power so the modulator and reconstruction filter stay synchronized. The digital outputs, however, must be recoded to allow for new signal levels for the split or zero samples. A simulation of all three dynamic delay methods was performed using a floating point accurate, 50% bandwidth, 3.35 MHz Gaussian pulse with −50 dB noise added. Fig. 9(A) shows the envelope-detected RF signal sampled at 214 MHz and normalized to the maximum signal amplitude. Digitizing the same RF signal with a 214 MHz, 2nd order delta-sigma A/D and reconstructing then envelope-detecting the result produces Fig. 9(B). The reconstructed noise level is higher than in the original signal because of the SQNR of the ΔΣ A/D.

Fig. 10 shows examples of the three extension techniques applied to the same RF signal. Fig. 10(A) shows the signal undergoing a delay change (sample repetition)

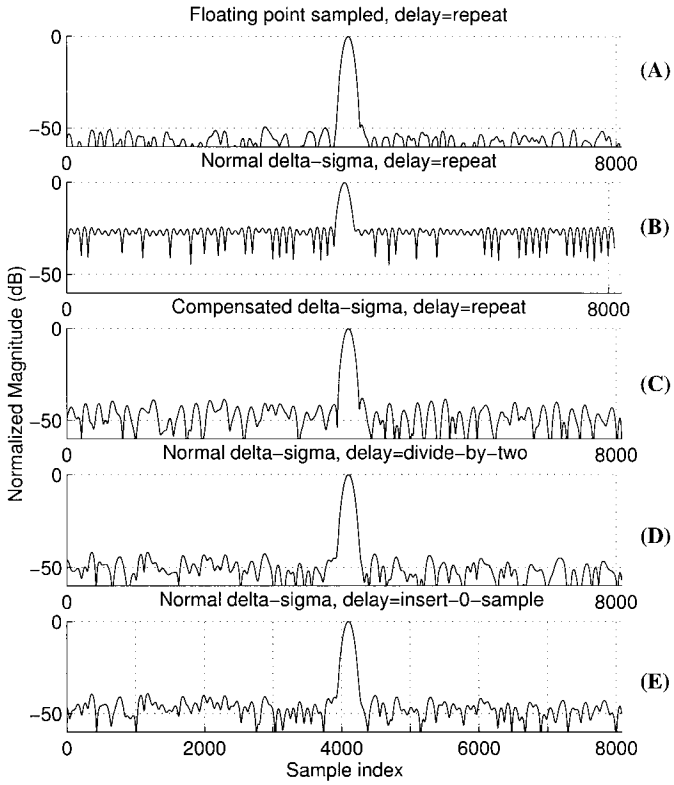

Fig. 10. Comparison of different sample manipulation techniques when delay change extends the sample stream.

every 200 sample points. Fig. 10(B) shows the same signal after passing through the 2nd order $\Delta\Sigma$ A/D and the sample repetition delay change. Degradation due to repeated samples is clearly evident in the increased noise level at a constant amplitude. Fig. 10(C) shows the result of a compensated $\Delta\Sigma$ A/D digitizing the signal prior to delaying it using repeated samples. The method of dividing every 200th sample in half to stretch the sample stream is shown in Fig. 10(D). Inserting a zero sample between every 200 normal $\Delta\Sigma$ samples is shown in Fig. 10(E).

The compensated $\Delta\Sigma$ signal [Fig. 10(C)] is considerably better than the uncompensated $\Delta\Sigma$ signal [Fig. 10(B)], although several small noise spikes are still perceptible. The divide-by-2 and insert zero techniques also yield delayed output signals considerably better than the uncompensated $\Delta\Sigma$ and slightly better than the compensated $\Delta\Sigma$ method. All three techniques come very close to the quantization noise level, shown previously in Fig. 9(B), which is the best that can be done (at this sampling rate). The actual performance of each technique is signal dependent and requires further in-depth study. The divide-by-2 and insert zero techniques are simpler than direct compensation because they require a simple digital recoding of the output samples to appropriately modify the delayed sample stream. Additionally, the analog multiplexer or multi-level DAC in the compensated $\Delta\Sigma$ modulator may introduce noise sources that could degrade system performance.

For digital recoding, the single bit output of the delta-sigma modulator, representing a $+1$ or -1, must be modified so that the new multi-bit digital value correctly represents the new levels needed for dynamic focusing. Adding a third, zero (0), level requires only one more bit in the digital word. The extra bit may be used to synthesize two different, yet equivalent, binary encodings shown in Table I. The divide-by-2 technique, however, requires two additional bits because of the position of these new levels between the $+1$ and -1 levels. An example of this coding is shown in Table II. One may note that the recoding methods are suitable to multi-beam operation, where several receive beams are generated simultaneously, whereas the compensated delta-sigma method is specific to only one beam.

Because of its simplicity and empirically equivalent performance, the unsigned insert zero technique is the preferred method of changing the dynamic receive delay in a digital $\Delta\Sigma$-based beamformer. Also, due to bit growth, it is better to perform the delay change (slip) at the output of the delay line so that the extra bit does not need to be carried through the structure.

There are also applications where the delay must be decreased [28], in which case there are two ways of compressing the sample stream: dropping a sample or summing it with the next sample. In both cases setting the output and feedback sample to zero, as shown in Fig. 8(B), correctly compensates the modulator and allows samples to be summed together or dropped in a straightforward manner. Dropping a sample is analogous to double incrementing a read pointer on a FIFO, in which the value of the dropped sample does not matter. The structure in Fig. 8(B) sets the dropped sample to zero; however, only the feedback path needs to be modified as in Fig. 8(A) because the sample to be dropped can be anything. The highlighted areas in Fig. 8 contain the multiplexer and 2x buffer and are the primary innovations of the compensated $\Delta\Sigma$ modulator.

All these methods vastly improve the quality of the final ultrasound image by ensuring that the modulator and demodulator remain synchronized on either side of the time variant delay change in the dynamic receive beamformer. Although simple, the effects of this modification are significant. Emulations using real ultrasound data are presented in Section VI that illustrate and quantify its effectiveness.

VI. Simulation Results

The Biomedical Ultrasonics Laboratory at the University of Michigan has acquired several complete ultrasound data sets from 128^2 transmit-receive measurements using a commercial 128 element, 3.5 MHz transducer (Acuson, Mountain View, CA, Model # V328) connected to a high speed digitizer [29]. These data allow any potential beamforming architecture to be emulated in software. For the specific tests presented here, images were generated of a wire target phantom, consisting of six wires in a water tank, and a cyst phantom, containing tissue mimicking gel with anechoic regions. The wires were aligned slightly away

TABLE I
DIGITAL RECODING TECHNIQUES FOR INSERTING A ZERO SAMPLE.

ΔΣ binary output	Digital level		ΔΣ binary output	Digital level	New coding Unsigned	New coding Signed
1	+1	→	1	+1	10 (2)	01 (1)
0	−1		0	−1	00 (0)	11 (−1)
			New Level	0	01 (1)	00 (0)

TABLE II
DIGITAL RECODING TECHNIQUES FOR DIVIDING A SAMPLE IN HALF.

ΔΣ binary output	Digital level		ΔΣ binary output	Digital level	New coding Unsigned	New coding Signed
1	+1	→	1	+1	100 (4)	010 (2)
0	−1		New level	+0.5	011 (3)	001 (1)
			New level	−0.5	001 (1)	111 (−1)
			0	−1	000 (0)	110 (−2)

from the transducer normal to prevent shadowing. These images can be used to compare spatial and contrast resolution produced by various beamforming architectures. The original ΔΣ-based beamformer, the preferred ΔΣ recoding beamformer, and a conventional, digital (10 bit A/D per channel) RF beamformer are compared, in which a low-pass second order modulator was used for both oversampled designs. A 222 MHz sampling rate was used for both oversampled systems, and a 13.9 MHz sample rate with an effective delay accuracy of 222 MHz was used for the conventional system. All wire target images are displayed over a 70 dB dynamic range, and all cyst images are displayed over a 50 dB dynamic range. These images were formed using a fully open transmit aperture focused at 60 mm and an unweighted receive aperture with a minimum F/number of two.

A. Wire Target Studies

In Section IV, we showed wire target images generated by the conventional and ΔΣ beamformers. Figs. 4 and 5 show the cross-section of the wires in the tank; however, Fig. 5 is degraded by a "snowy" noise background. The noise, primarily due to delay switching, is at a level approximately 55 dB below that of the strongest wire reflector (third from the top). Blood flow detection, including Doppler or color mode imaging, would be impossible using such a system because blood-related signals often lie about 70 to 80 dB below the brightest tissue reflection.

The images in Figs. 6 and 7 are derived from the same architectures, but with fixed delays so that dynamic delay switching is eliminated. Reduced resolution and distorted point spread functions result from the systems being out of focus, except at 60 mm (near the third wire). The background noise, however, is the important characteristic of Fig. 7 because it is much closer in magnitude to the background of the 10-bit RF fixed focus beamformed image shown in Fig. 6. The noise floor in Fig. 7 is due solely to the ΔΣ modulation efficiency imposed by the oversampling ratio of the system. That is, the noise floor in this image results from ΔΣ modulation noise shaping, not delay changes as in Fig. 5. Increased sampling frequency or higher order ΔΣ modulators could be used to further reduce the noise present in this image.

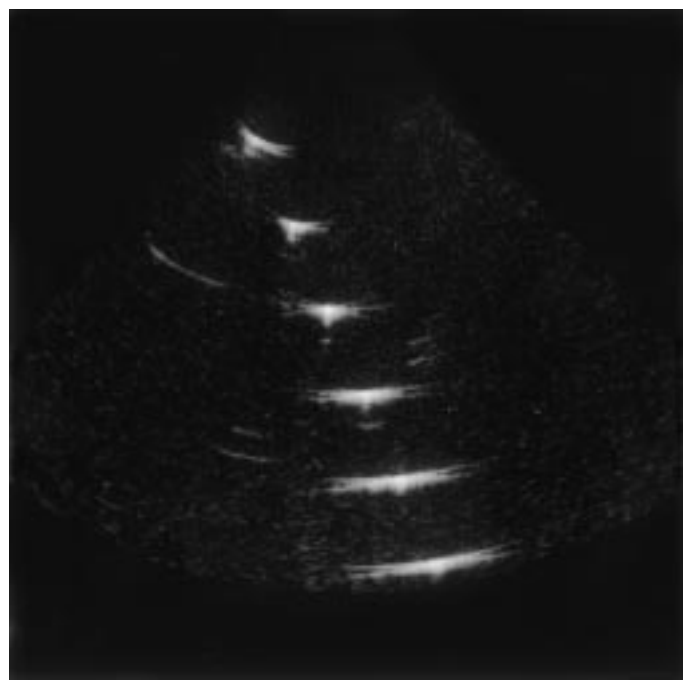

Fig. 11. Insert-zero ΔΣ-delay-sum beamformer with dynamic focusing. Target: wire phantom.

Fig. 11 presents an image generated by a dynamically focused, zero-insertion recoding, ΔΣ beamformer. Comparing this to Fig. 4, both have equivalent point-spread functions at each wire. Acoustic artifacts near the

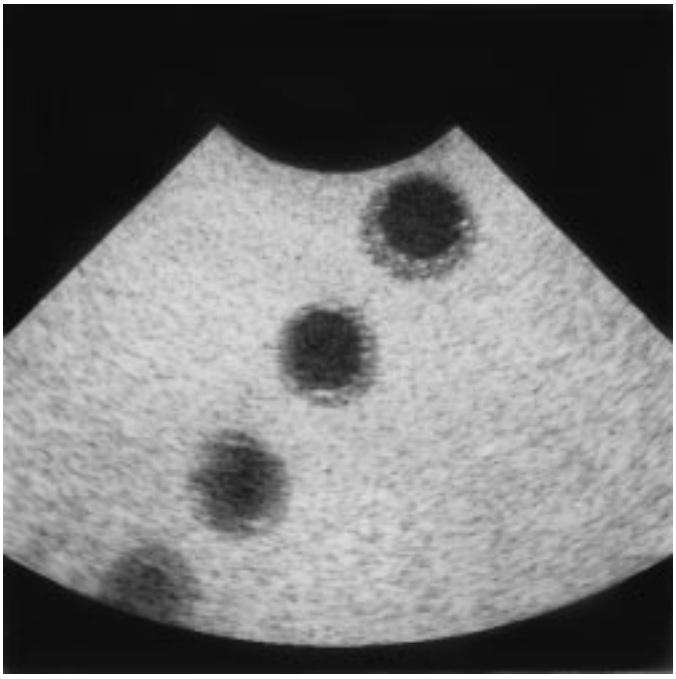

Fig. 12. Uncompensated $\Delta\Sigma$-delay-sum beamformer with dynamic focusing. Target: cyst phantom.

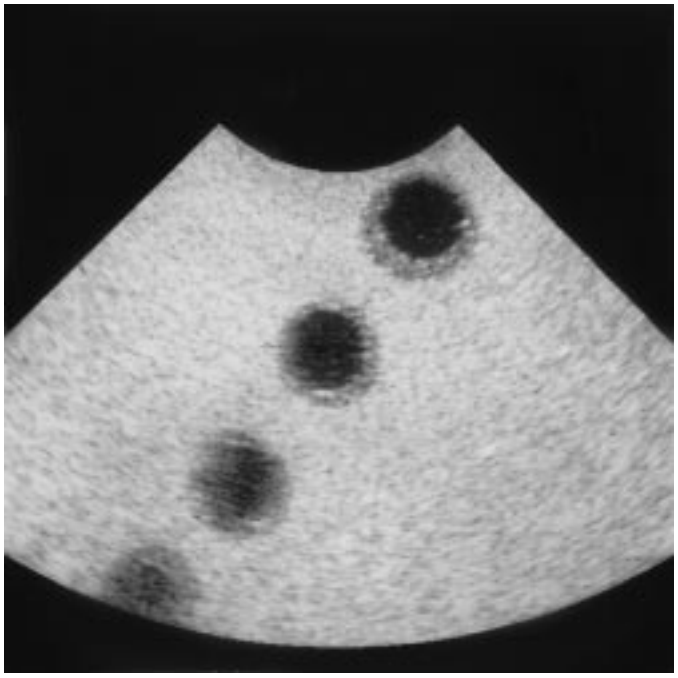

Fig. 13. Insert-zero $\Delta\Sigma$-delay-sum beamformer with dynamic focusing. Target: cyst phantom.

central wires, probably due to air bubbles in the water, are visible in both images. The background noise in the recoded $\Delta\Sigma$ based system is roughly the same as the fixed focus $\Delta\Sigma$ beamformed image in Fig. 7. Remember that this background noise is due to the $\Delta\Sigma$ modulation noise shaping efficiency, not delay changes in the beamformer. Clearly, the recoding $\Delta\Sigma$ beamformer structure proposed here almost completely eliminates noise generated by dynamic focusing delay changes. The noise floor in the $\Delta\Sigma$ image lies about 72 dB below the strongest point reflector. This high quality image rivals the resolution and signal-to-noise ratios currently available in midrange to top-of-the-line clinical ultrasound scanners. Color flow processing can be done using this compensated $\Delta\Sigma$ beamformer because its noise floor is sufficient to detect low intensity blood signals.

B. Cyst Phantom Studies

A similar set of images as those presented here were generated using cyst phantom data. Fig. 12 was beamformed using an uncompensated $\Delta\Sigma$ modulator and repeating delays. Fig. 13, however, was generated using the proposed insert-zero $\Delta\Sigma$ beamformer. The cysts are less pronounced in the uncompensated version (Fig. 12). Noise degrading the background in Fig. 5 fills in anechoic regions of the uncompensated $\Delta\Sigma$ image, thus decreasing contrast and cyst detectability. The insert-zero $\Delta\Sigma$ image is nearly identical to the traditionally beamformed image, shown in Fig. 14.

To quantify contrast resolution performance for the various architectures, the contrast to noise (CNR) can be

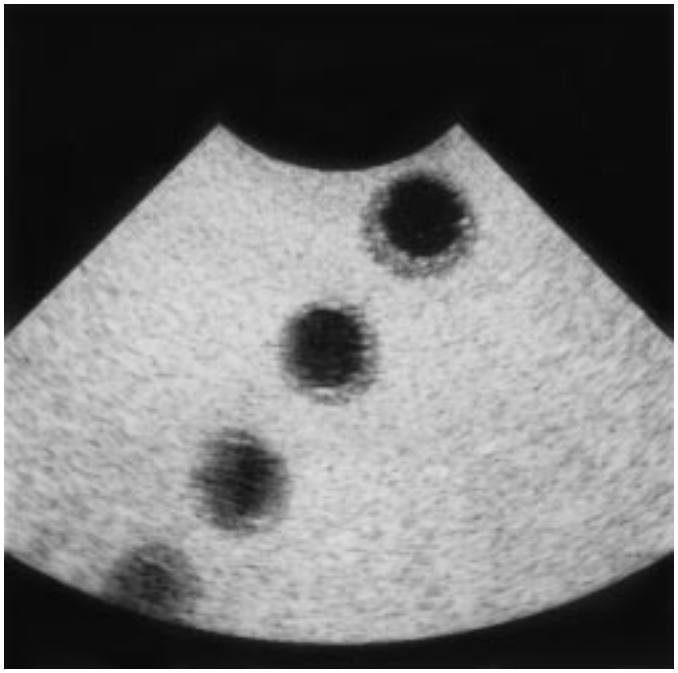

Fig. 14. Ten-bit A/D-delay-sum beamformer with dynamic focusing. Target: cyst phantom.

TABLE III
CONTRAST TO NOISE RATIO (CNR) FROM EACH OF THE BEAMFORMING ARCHITECTURES IN ANECHOIC REGIONS OF THE CYST IMAGES.

Beamforming method	Contrast-to-Noise Ratio (CNR) Cyst #1	Cyst #2	Cyst #3
Uncompensated $\Delta\Sigma$	4.72	4.64	3.68
Compensated $\Delta\Sigma$	5.53	5.06	3.88
Divide-by-2 $\Delta\Sigma$	5.55	5.06	3.90
Insert-0 $\Delta\Sigma$	5.55	5.07	3.90
Traditional	5.58	5.07	3.90

measured for each anechoic region. The CNR is defined as:

$$\mathrm{CNR} = \frac{|\mu_{\mathrm{out}} - \mu_{\mathrm{in}}|}{\sigma_{\mathrm{out}}}, \tag{6}$$

where μ_{out} and μ_{in} are the mean values outside and inside the cyst regions, and σ_{out} is the standard deviation outside the cysts [29]. The measurements inside the cysts took into account most of each anechoic region, and the measurements outside the cysts consisted of large rectangles at the same ranges as each cyst. Results for all architectures are presented in Table III.

These CNR values indicate that the recoding $\Delta\Sigma$ beamforming techniques and the traditional beamformer generate images with roughly equivalent contrast resolution and detectability. It is also interesting to note that the difference between the uncompensated and traditional methods varies as a function of depth. As depth increases, the uncompensated $\Delta\Sigma$ beamformer appears to undergo less noise degradation. This is because the rate of delay changes decreases as a function of 1/Range. Near the top of the image, close to the transducer, delays change rapidly, injecting considerable noise. Toward the bottom of the image delays change infrequently, thus injecting less noise.

Implementing the 2X buffer in the compensated $\Delta\Sigma$ depends on the technology used for the rest of the modulator. Scaling an analog signal by two may vary from process to process or wafer to wafer. Consequently, the effects of these variations on the compensated $\Delta\Sigma$ beamformer must be quantified. As an initial test, we investigated the effects of a nonideal 2X buffer that fed back only 1.7X the normal value. An image of the wire target phantom produced with this defect is presented in Fig. 15. Although the noise floor is slightly worse (roughly 5.5 dB higher), the image quality is still substantially better than the uncompensated version. Therefore, the method of compensating the $\Delta\Sigma$ modulator for changing delays is robust against process variations affecting the 2X feedback scaling buffer.

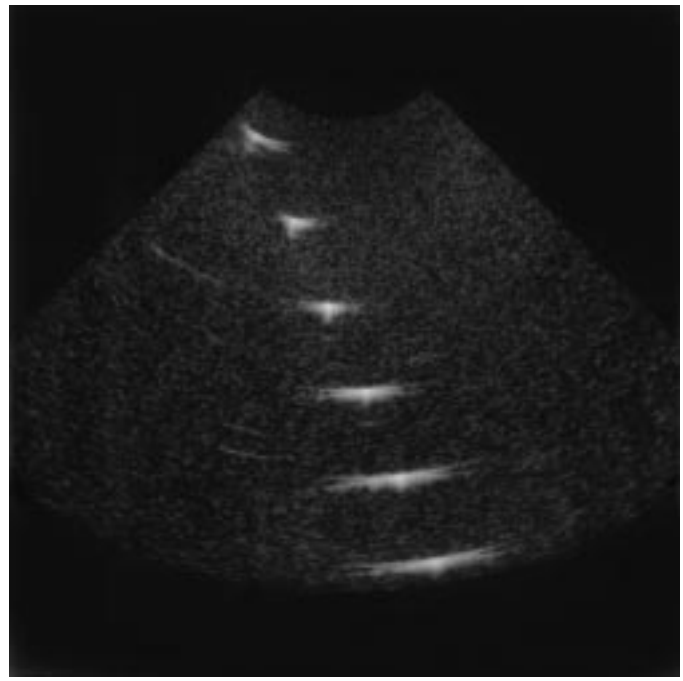

Fig. 15. Dynamically focused, compensated, $\Delta\Sigma$-delay-sum method with a 1.7X buffer rather than an ideal 2X buffer for feedback path.

VII. DISCUSSION

The $\Delta\Sigma$ digital beamforming method originally proposed by General Electric [18] and discussed in this paper suffers from noise artifacts injected by delay changes necessary for dynamic receive focusing. This artifact has been successfully eliminated by modifying the modulator or recoding the delayed samples so that the modulators and demodulator of the system remain synchronized. Images generated by the corrected $\Delta\Sigma$ beamformers are comparable in quality to those using traditional multi-bit digital RF beamformers. In addition, the $\Delta\Sigma$ based oversampling technique has the potential for significant reduction in power consumption and size of the dynamic receive beamformer. Recent work by several groups suggests that portable ultrasound scanners with a real-time beamformer fully integrated into the probe head are commercially viable[3] [30]. The $\Delta\Sigma$ architecture presented in this paper may be well suited to such a system.

Although $\Delta\Sigma$-based beamforming can generate images of good quality, it is unclear at this time what the power savings are compared to traditional beamformers. A key power issue is the increased sampling rate. Because power consumption of CMOS circuits is directly proportional to the switching frequency, a factor of six increase in clock frequency may cause a significant power consumption increase [31]. Offsetting this apparent disadvantage is the impressive simplicity of the circuitry. The $\Delta\Sigma$ A/D on every channel has roughly 100 times fewer analog components (perhaps 10 active components versus 1,024 comparators and a biasing network). The delay circuits, to be implemented with a digital dynamic FIFO with variable read-to-write pointer offsets, are very similar in structure and size to the traditional coarse delay means. However, the $\Delta\Sigma$ beamformer does not have any of the per-channel interpolate-decimate or baseband-rotate struc-

[3] http://web-ext2.darpa.mil/DSO/rd/UltraSnd/index.html - DARPA ultrasound projects.

tures required in slower, traditional architectures. The physical size of this beamformer when fabricated with deep submicron processes will thus be a significant improvement over traditional means. It is expected that about 32 to 64 channels of the complete beamformer can be fabricated on a single chip. Therefore, even though power consumption is uncertain at this time, its simplicity and size improvements over traditional methods indicate that it is a potential means of creating very high channel count or portable systems.

Another potential disadvantage of designs exploiting oversampling is their decreasing sensitivity (i.e., SQNR) as the ultrasound carrier frequency increases. Most systems today can accept transducers ranging from 2 to 10 MHz. Their beamformers likewise are able to process signals from these transducers with little loss in sensitivity. Provided they use a fixed sampling frequency, these systems would suffer a 7 dB loss in sensitivity, as given by (1), for a five times reduction in oversampling ratio. A first order delta-sigma modulator, however, would suffer a 20 dB loss in sensitivity given the same increase in carrier frequency with a fixed sampling frequency, according to (3). A second and third order modulator would suffer a 35 and 48 dB loss, respectively. To extend oversampling methods to higher signal frequencies, we are exploring simple circuit modifications incorporating analog mixing of the input waveform as part of the basic modulator structure. The mixer (or premodulator as we call it) will shift the frequency of the ultrasound signal toward DC, where the $\Delta\Sigma$ modulator performs better. For narrow bandwidth high frequency signals, this method is particularly useful because considerable frequency heterodyning can be effected without causing carrier sideband mingling. Another promising area where this premodulation technique may be useful is to increase Doppler sensitivity. Since most Doppler imaging is done with narrow band pulses, frequency heterodyning can yield a 20 to 40 dB improvement in Doppler sensitivity. A future paper will address this technique in detail and present simulation results demonstrating improved Doppler sensitivity.

References

[1] M. O'Donnell, "Applications of VLSI circuits to medical imaging," *Proc. IEEE*, vol. 76, pp. 1106–1114, Sep. 1988.

[2] C. F. Schueler, H. Lee, and G. Wade, "Fundamentals of digital ultrasonic imaging," *IEEE Trans. Sonics Ultrason.*, vol. SU-31, pp. 195–217, July 1984.

[3] O.T. von Ramm and S. W. Smith, "Beam steering with linear arrays," *IEEE Trans. Biomed. Eng.*, vol. BME-30, pp. 438–452, Aug. 1983.

[4] S. H. Maslak, "Acoustic imaging apparatus," U.S. Patent 4,140,022, February 20, 1979.

[5] S. H. Maslak and J. N. Wright, "Phased array acoustic imaging system," U.S. Patent 4,550,607, November 5, 1985.

[6] M. O'Donnell, W. E. Engeler, J. T. Pedicone, A. M. Itani, S. E. Noujaim, R. J. Dunki-Jacobs, W. M. Leue, C. L. Chalek, L. S. Smith, J. E. Piel, R. L. Harris, K. B. Welles, and W. L. Hinrichs, "Real-time phased array imaging using digital beam forming and autonomous channel control," *Proc. IEEE Ultrason. Symp.*, 1990, pp. 1495–1498.

[7] R. G. Pridham and R. A. Mucci, "Digital interpolation beamforming for low-pass and bandpass signals," *Proc. IEEE*, vol. 67, pp. 904–919, June 1979.

[8] D. Lipschutz, "Delay interpolator for digital phased array ultrasound beamformers," U.S. Patent 5,345,426, September 6, 1994.

[9] M. O'Donnell and M. G. Magrane, "Method and apparatus for fully digital beam formation in a phased array coherent imaging system," U.S. Patent 4,809,184, February 28, 1989.

[10] M. O'Donnell, W. E. Engeler, T. L. Vogelsong, S. G. Karr, and S. E. Noujaim, "Method and apparatus for high speed digitial phased array coherent imaging system," U.S. Patent 4,839,652, June 13, 1989.

[11] R. E. Davidsen and S. W. Smith, "Sparse geometries for two-dimensional array transducers in volumetric imaging," *Proc. IEEE Ultrason. Symp.*, 1993, pp. 1091–1094.

[12] P. C. Li and M. O'Donnell, "Elevational spatial compounding," *Ultrason. Imaging*, vol. 16, pp. 176–189, 1994.

[13] D. G. Wildes, R. Y. Chiao, C. M. Daft, K. W. Rigby, L. S. Smith, and K. E. Thomenius, "Elevation performance of 1.25D and 1.5D transducer arrays," *IEEE Trans. Ultrason., Ferroelect., Freq. Contr.*, vol. 44, pp. 1027–1037, Sep. 1997.

[14] G. R. Lockwood, P.-C. Li, M. O'Donnell, and F. S. Foster, "Optimizing the radiation pattern of sparse periodic linear arrays," *IEEE Trans. Ultrason., Ferroelect., Freq. Contr.*, vol. 43, pp. 7–14, Jan. 1996.

[15] G. R. Lockwood and F. S. Foster, "Optimizing the radiation pattern of sparse periodic two-dimensional arrays," *IEEE Trans. Ultrason., Ferroelect., Freq. Contr.*, vol. 43, pp. 15–19, Jan. 1996.

[16] J. C. Candy and G. C. Temes, *Oversampling Delta-Sigma Data Converters—Theory, Design, and Simulation*. IEEE Press, Piscataway, NJ, 1992.

[17] S. R. Norsworthy, R. Schreier, and G. C. Temes, *Delta-Sigma Data Converters—Theory, Design, and Simulation*. IEEE Press, Piscataway, NJ, 1997.

[18] S. E. Noujaim, S. L. Garverick, and M. O'Donnell, "Phased array ultrasonic beam forming using oversampled A/D converters," U.S. Patent 5,203,335, April 20, 1993.

[19] M. Dean, "Digital beamforming array," U.S. Patent 5,461,389, October 24, 1995.

[20] L. Gwennap, "Digital's 21164 Reaches 500 MHz," *Microprocess. Rep.*, vol. 10, July 8, 1996.

[21] L. A. Williams and B. A. Wooley, "Third-order cascaded sigma-delta modulators," *IEEE Trans. Circuits Syst.*, vol. 38, pp. 489–497, May 1991.

[22] R. M. Gray, "Quantization noise spectra," *Trans. Information Theory*, vol. IT-36, pp. 1220–1244, Nov. 1990.

[23] S. H. Maslak, "Computed sonography," in *Ultrasound Annual 1985*. Raven Press, NY: 1985.

[24] D. K. Peterson and G. S. Kino, "Real-time digital image reconstruction: A description of imaging hardware and an analysis of quantization errors," *IEEE Trans. Sonics Ultrason.*, vol. SU-31, pp. 337–351, July 1984.

[25] G. F. Manes, C. Atzeni, and C. Susini, "Design of a simplified delay system for ultrasound phased array imaging," *IEEE Trans. Sonics Ultrason.*, vol. SU-30, pp. 350–354, Nov. 1983.

[26] Y. H. Hu, "CORDIC-Based VLSI architectures for digital signal processing," *IEEE Signal Processing*, pp. 16–35, July 1992.

[27] O. Norman, "A band-pass delta-sigma modulator for ultrasound imaging at 160 MHz clock rate," *IEEE J. Solid-State Circuits*, vol. 31, pp. 2036–2041, Dec. 1996.

[28] A. Macovski, "Ultrasonic electronic lens with reduced delay range," U.S. Patent 4,058,003, November 15, 1977.

[29] M. Karaman, P. C. Li, and M. O'Donnell, "Synthetic aperture imaging for small scale systems," *IEEE Trans. Ultrason., Ferroelect., Freq. Contr.*, vol. 42, pp. 429–442, May 1995.

[30] A. M. Chiang and S. R. Broadstone, "Portable ultrasound imaging system," U.S. Patent 5,590,658, January 7, 1997.

[31] N. Weste and K. Eshragian, *Principles of CMOS VLSI Design, A Systems Perspective*. Reading, MA: Addison Wesley, June 1988, pp. 119–158, Chapter 4.

Steven R. Freeman (S'93–M'98) attended the University of Michigan and received his B.S.E, M.S.E, and Ph.D. in electrical engineering in 1991, 1994, and 1998, respectively. As an undergraduate, he developed instrumentation for high energy gamma ray astronomy and was a member of the solar car team. His graduate research at the University was concerned with oversampled ultrasound beamformers for low-power, portable scanners. This research interest continues to be his primary focus as an employee of Q-DOT Inc., Colorado Springs, CO. Dr. Freeman is also interested in digital circuit design and signal processing.

Marshall Quick received his bachelor's degree in electrical engineering from Princeton University in 1969 and an MSEE from Syracuse University in 1974. From 1969 to 1994, he was an engineer at General Electric and Martin Marietta, Utica, NY, where he designed several analog charge coupled device signal processors, and cryogenic focal plane readout circuits for infrared detector arrays. In 1994 Mr. Quick joined Q-Dot, Inc., Colorado Springs, CO, where he is involved in the design of analog CMOS and CCD signal processor integrated circuits, primarily for ultrasound and sonar applications.

Marc A. Morin (S'88–M'92) received his B.S.E.E. Summa Cum Laude in 1990 and M.S.E.E. in 1992 from the University of New Hampshire. While attending the University of New Hampshire, Mr. Morin was a test engineer for General Electric Company, Somersworth, NH. Later, he was a lead DSP software design engineer for NAVSYS Corporation, Colorado Springs, CO, developing advanced GPS receiver systems. He then joined Q-DOT, Inc., Colorado Springs, CO, where he has developed advanced monolithic HBT integrated circuits, including high speed, high-resolution data converters and RF circuits. Mr. Morin is presently employed at Atmel Corporation in Colorado Springs, CO, developng integrated circuits for software radios. His research interests include mixed-mode and multi-rate signal processing systems for advanced audio and radio-frequency equipment. He is also a member of Tau Beta Pi.

Charles S. Desilets (S'75–M'77) received his B.S. and M.S. degrees in engineering physics from The Ohio State University in 1969. He was employed at Bell Telephone Laboratories for 4 years before re-entering graduate school at Stanford University, where he received his Ph.D. in electrical engineering in 1978. During his sojourn at Stanford, he conducted research into ultrasonic transducers and arrays and published several papers on phased array element and quarter-wave matching layer design. He founded in 1978 and served as president of Precision Acoustic Devices, Inc., a company that manufactured ultrasonic transducers for medical and industrial applications. The company was sold to Advanced Technology Laboratories in 1990, and Dr. Desilets served three years as Director of Scanhead Technology at ATL. In 1993, Dr. Desilets established a consulting practice, UltraSound Solutions, which provides expertise in the design, development, and manufacture of ultrasonic transducers and arrays for imaging, therapeutic, sonar, and Doppler applications. In 1996, UltraSound Solutions was incorporated as Ultrex Corporation, an organization that conducts development of advanced ultrasound technologies.

Matthew O'Donnell (M'79–SM'84–F'93) received the B.S. and Ph.D. degrees in physics from the University of Notre Dame, Notre Dame, IN, 1972 and 1976, respectively.

Following his graduate work, he moved to Washington University in St. Louis as a postdoctoral fellow in the Physics Department working on applications of ultrasonics to medicine and non-destructive testing. He subsequently held a joint appointment as a Senior Research Associate in the Physics Department and a Research Instructor of Medicine in the Department of Medicine at Washington University. In 1980 he moved to General Electric Corporate Research and Development in Schenectady, New York, where he continued to work on medical electronics, including NMR and ultrasound imaging systems. During the 1984–1985 academic year, he was a visiting fellow in the Department of Electrical Engineering at Yale University investigating automated image analysis systems. Most recently, he has worked on the application of advanced VLSI circuits to medical imaging systems, including catheter arrays. In a bold move during 1990, Dr. O'Donnell moved to the Electrical Engineering & Computer Science Department at the University of Michigan in Ann Arbor, Michigan, where he is currently a Professor.

Dr. O'Donnell is a member of Sigma Xi, the American Physical Society, and is a fellow of both the IEEE and the AIMBE. He has authored or coauthored over 100 archival publications, including 2 receiving best paper awards, numerous presentations at national meetings, and 37 patents.